Applied Energy 235 (2019) 786–801

Contents lists available at ScienceDirect

Applied Energy

journal homepage: www.elsevier.com/locate/apenergy

A hybrid forecasting system based on fuzzy time series and multi-objective optimization for wind speed forecasting

Ping Jiang, Hufang Yang*, Jiani Heng

School of Statistics, Dongbei University of Finance and Economics, Dalian, China

HIGHLIGHTS

- Develop a novel hybrid forecasting system including three modules.
- Balance the forecast accuracy and stability simultaneously in forecasting.
- Optimize the cut points and weight in fuzzy time series method.
- Consider the different time intervals of wind speed data in actual practice.

ARTICLE INFO

Keywords:
Wind speed forecasting
Multi-objective differential evolution
Weighted fuzzy time series
Comprehensive evaluation

ABSTRACT

Wind speed forecasting is fundamental to the dispatching, controllability, and stability of the power grid. As a challenging but essential work, wind speed forecasting has attracted significant attention from researchers and managers. However, traditional forecasting models sometimes fail to capture data features owing to the randomness and intermittency of wind speed, and the models always focus only on improving accuracy, which is one-sided. Motivated by these problems, in this study, a novel hybrid forecasting system consisting of three modules (a data preprocessing module, optimization module, and forecasting module) is developed to improve the forecasting accuracy and stability. In the data preprocessing module, an effective denoising technique is used to produce a smoother sequence. A fuzzy time series method optimized by a multi-objective differential evolution algorithm that balances the conflict between forecasting accuracy and stability is developed in the next two modules to perform the forecasting. Several experimental results covering different models and wind-speed time intervals all indicate that our proposed hybrid forecasting system can achieve both satisfactory accuracy and stability with a mean absolute percentage error of below 4% in wind speed forecasting. Moreover, the statistical hypothesis test, forecasting effectiveness and grey relational degree are discussed which also demonstrate the great performance of proposed system.

1. Introduction

Energy is a crucial material basis for human social progress and economic development that influences all aspects of social life. Traditional energy sources such as coal and oil are not only limited in availability, but also cause significant environmental pollution [1]. Doubtless, the goal of mitigating the energy crisis and reducing traditional environmental pollution must be achieved through accelerating

Abbreviations: AIC, A-information criterion; ANFIS, adaptive neuro-fuzzy inference system; ANN, artificial neural network; ARIMA, autoregressive integrated moving average; BPNN, back propagation neural network; CS, cuckoo search; DA, direction accuracy; DE, differential evolution; DES, double exponential smoothing; DM, Diebold-Mariano; EEMD, ensemble empirical mode decomposition; EF, equal frequency; ELM, extreme learning machine; EMD, empirical mode decomposition; EW, equal width; FA, firefly algorithm; FE, forecasting effectiveness; FEEMD, fast ensemble empirical mode decomposition; FLR, fuzzy logical relationship; FNN, feed-forward neural network; FTS, fuzzy time series; GA, genetic algorithm; GRD, grey relational degree; GW, gigawatts; GWEC, global wind energy council; HS, harmony search; LHS, left-hand side; MAE, mean absolute error; MAPE, mean absolute percentage error; MARS, multivariate adaptive regression spline; MODE, multi-objective differential evolution; MOEA, multi-objective evolution algorithm; NRM, nonparametric regression model; NWP, numerical weather prediction; PSO, particle swarm optimization; RBFNN, radial basis function neural network; RHS, right-hand side; RMSE, root mean square error; SVM, support vector machine; SVR, support vector regression; TIC, Theil inequality coefficient; VAR, variance of the forecasting error; WNN, wavelet neural network; WPD, wavelet packet decomposition

* Corresponding author.
E-mail address: dufeyang_16@163.com (H. Yang).

https://doi.org/10.1016/j.apenergy.2018.11.012
Received 23 May 2018; Received in revised form 16 August 2018; Accepted 6 November 2018
0306-2619/

the adjustment of the energy structure, which makes the development of new energies the key point [2].

In recent years, the development of renewable energy has gradually become the consensus of the international community [3]. Many countries have listed the development of renewable energy in their energy development strategies, and regarded promoting the development of renewable energy as a major measure to guarantee the sustainable development of humanity, the society, and the economy. In new energy fields, wind power is an important part of the new energy industry and has great significance for optimizing the energy structure and realizing energy savings and emission reductions [4]. According to the Paris Agreement, a decarbonized electricity supply is supposed to be completely popularized before 2050, and wind power plays a vital role in achieving this goal.

With improvements in wind power technology, the wind power industry has developed rapidly. The Global Wind Energy Council (GWEC) released its annual statistics report about the global wind energy industry. The report reveals that in 2016, a total of up to 54 GW (gigawatts) worth of wind energy was brought online, and accordingly a cumulative total of nearly 487 GW in global wind energy was achieved. The GWEC also published a biennial Global Wind Energy Outlook, which indicated that up to 20% of global electricity could be supplied by wind power by 2030. Moreover, by 2030, wind power could reach 2110 GW, creating 2.4 million new job opportunities, reducing more than 3.3 billion tons of CO_2 emissions per year, and attracting investments of about €200 billion annually [5].

Wind energy resources in China are rich, and the total reserves are about 3.226×10^5 MW. The available wind energy reserves on land are 2.53×10^5 MW, which is a prerequisite for the rapid development of China's wind power industry [6]. According to the GWEC, a total of up to 23 GW of wind energy in 2016 is installed in China, nearly half the 54 GW of total global wind energy was brought online, and this continued to expand to lead the nearest competitors such as the United States and Germany [7].

As the proportion of wind power generation in the power system increases gradually, the safe and stable operation of the power system must be affected by wind power [8]. Different from traditional power generation modes, the generation of wind power depends on the existence of wind, but the stochastic and intermittent characteristics of wind result in a greater randomness and volatility of wind power, which greatly increases its uncontrollability [9].

Therefore, in order to ensure the stable and safe operation of the power system and promote further development of the wind power industry, it is necessary to effectively improve the controllability and predictability of wind power. As the crucial influencing factor of wind power, wind speed forecasting can provide a very important reference for relevant sectors and managers with regard to wind power integration and power dispatching. Accurate forecasting of wind speed on a wind farm can foresee the variety of wind speeds so that the controllability of wind power generation can be improved and adverse effects caused by wind power integration on the grid can be effectively mitigated [10]. Nowadays, research studies about wind speed forecasting are drawing more and more concern from scholars and managers, and various models have been developed for wind forecasting. These models can be divided into physical, statistical, and artificial intelligence types [11].

1.1. Physical forecasting models

The physical forecasting model, a numerical weather prediction (NWP), uses forecast results of the weather forecasting system including wind speed, wind direction, temperature, and other weather data [12]. The contours, obstacles, and other physical information around measurement points are integrated in real time [13]. A very-short-term forecasting method was proposed by Gao [14] combining chaos phase space reconstruction with NWP, and the results indicated that the proposed method had an improved forecasting accuracy. A physical model can achieve good performance in long-term forecasting but is sensitive to market information and will consume a large amount of computing resources [15].

1.2. Statistical forecasting models

Comparing with physical models, traditional statistical models and artificial intelligence models are more widely used in the literature. The Autoregressive Integrated Moving Average (ARIMA) method is one of the typical statistical models. For the ARIMA (p, d, q) method, p is an autoregressive term, q is a moving average term, and d is the number of differences made when the time series becomes stationary. The f-ARIMA was applied by Rajesh et al. [16] to forecast day-ahead and two-day-ahead wind speeds, and ARIMA was used by Radziukynas et al. [17] to forecast the short-term wind speed of a wind farm in Lithuania. The results indicated that good forecasting performance results were all obtained by them. A hybrid ARIMA-ANN (artificial neural network) model was proposed by Cadenas [18] to simulate the average hourly wind speed in three different regions of Mexico. In addition to ARIMA, the rise of other statistical forecasting models attracted more research attention. These models include the nonparametric regression model (NRM) [19] and double exponential smoothing (DES) [20].

1.3. Artificial intelligence models

Statistical models have wide application and require less time to build, but the forecasting results are always inaccurate owing to the nonlinearity and high volatility of the wind speed data. Therefore, artificial intelligence models were developed to overcome some of these limitations. The forecasting performance of ARIMA and ANN were compared by Chen et al. [21] for the hourly wind speed. The results demonstrated that the ANN model performed more effectively than the ARIMA model in forecasting the short-term hourly wind speed. A Kalman filter was hybridized with an ANN by Shukur et al. [22] based on ARIMA to handle the stochastic uncertainty for more accurate wind speed forecasting. An empirical mode decomposition (EMD)-based feed-forward neural network (FNN) ensemble learning paradigm model was proposed by Guo et al. [23] for multistep wind speed forecasting. The proposed model showed better performance than the basic FNN.

1.4. Hybrid forecasting model

Artificial intelligence models can achieve good results, but they also have some shortcomings such as a difficulty in parameter determination and computational complexity. To improve the process and performance of wind speed forecasting, some hybrid models have been developed. One type of hybrid model conducts data preprocessing before forecasting. Examples of this type are the EEMD (ensemble empirical mode decomposition)-CS (cuckoo search)-WNN (wavelet neural network) [24] and the WPD (Wavelet Packet Decomposition)-FEEMD (Fast Ensemble Empirical Mode Decomposition)-Elman [25].

Another common hybrid model applies an optimization algorithm to search the best parameters of forecasting models. Examples include the CS-SVM (support vector machine) [26], GA (genetic algorithm)-RBFNN (Radial Basis Function neural network) for short-term wind power forecasting, and PSO (Particle Swarm Optimization)-MARS (Multivariate Adaptive Regression Spline) [27]. The hybrid models that combine data preprocessing and an optimal algorithm can achieve better forecasting accuracy than previous methods. In addition to the above two types of methods, there are other hybrid methods. For example, ARIMA was used to find the best structure of an ANN model and initialize the state equations of a Kalman model [28]. The adaptive neuro-fuzzy inference system (ANFIS) combined with an ANN was applied by Okumus [29] for wind speed forecasts. The results all showed that the proposed model could achieve better performance for all

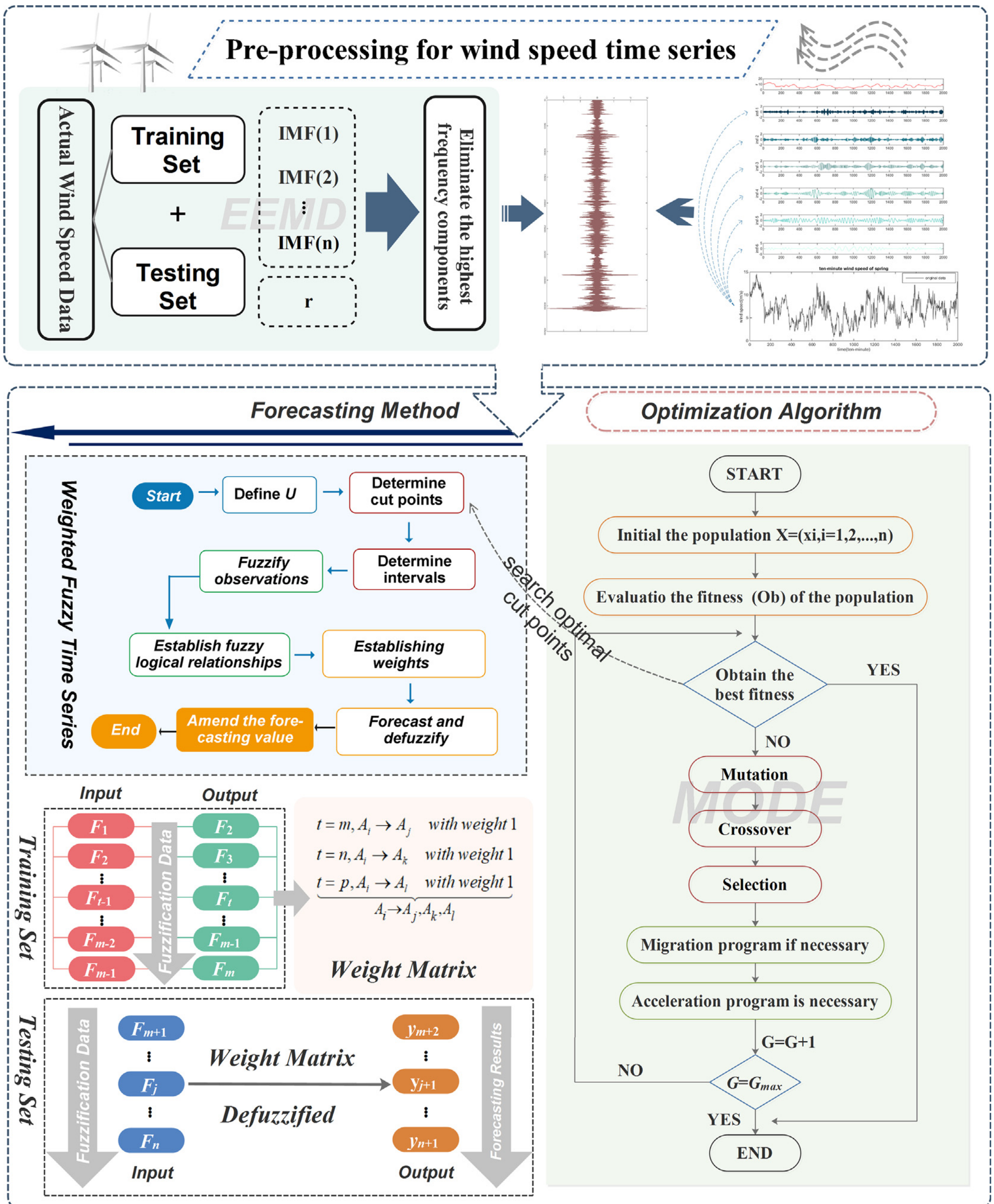

Fig. 1. Structure of our proposed hybrid forecasting system.

datasets.

1.5. Proposed forecasting system

Based on the above analysis, the optimal algorithm in most previous research studies concentrated only on improving the forecasting accuracy, while the status of forecasting stability, which also played a crucial role in wind speed forecasting, was ignored [30]. Therefore, in order to take objectives such as accuracy and stability into consideration, the multi-objective evolution algorithm (MOEA) was first proposed by Schaffer [31]. New MOEAs have been developed in several fields such as the multi-objective genetic algorithm [32], multi-objective particle swarm optimization [33], and multi-objective bat algorithm [34].

Thus, to overcome the instability of wind speed data which may cause the poor forecasting performance for wind speed, a novel hybrid forecasting system is developed in this paper for wind speed forecasting to obtain both better accuracy and good stability of forecasting results. This system includes three modules: a data preprocessing module, optimization module, and forecasting module. In the data preprocessing module, based on the "decomposition and ensemble" strategy, the wind speed data can be decomposed into several intrinsic mode functions. Then, the highest-frequency signal namely noise is eliminated to reduce volatility and the rest signals are assembled to obtained new time series for forecasting. Among the forecasting, the multi-objective differential evolution (MODE) algorithm is developed to search the optimal cut points and weights in the amended equation of the Fuzzy Time Series (FTS) algorithm which is the main forecasting method for wind speed time series. In FTS, continuous values are constructed into several fuzzy sets and discrete values according to the cut points obtained by MODE. Then a weight matrix is determined by fuzzy logical relationships for further forecasting step. Finally, the final forecasting results are obtained by defuzzification method. Accordingly, the characteristics and main contributions of our paper are as follows:

A novel hybrid forecasting system including a data preprocessing module, optimization module, and forecasting module are developed in our study. Compared with competitive models, in our proposed system, the high volatility and instability of wind speed time series are well overcome to some degree and greater forecasting performance can be achieved demonstrated by several experiments.

A multi-objective differential evolution algorithm is proposed which focuses on balancing the forecast accuracy and stability simultaneously. To achieve both accurate and stable results for wind speed forecasting, multi-objective differential evolution is proposed to optimize the cut points and weights of fuzzy time series to remedy the shortcomings of single-objective optimization algorithms, which only can consider one objective and neglect other crucial aspects.

In different productive activities, the intervals of the wind speed time series forecasting are various according to different demand of the managers. Thus, in this paper, three different time horizon wind speed time series (10 min, 30 min, and 60 min) are selected for further discussion to meet different requirement in actual application. The results comprehensively verify the practicability and universality of our proposed system for wind speed forecasting.

A scientific and thorough test and evaluation system is created to assess the performance of our proposed system. Three testing methods [Diebold-Mariano (DM) test, forecasting effectiveness (FE), and Grey relational degree (GRD)] and six evaluation indicators containing three aspects (accuracy, stability, and future change forecasting) are developed for comprehensive comparison between our proposed system and other competitive models.

The rest of this paper is organized as follows: The main methods and proposed forecasting system for our proposed system are introduced in Section 2. The experimental results from different aspects are analyzed in Section 3, while the results comprehensively are further discussed in Section 4. Conclusion is given in Section 5. Structure of our proposed hybrid forecasting system including three parts (data pre-processing, optimization algorithm and forecasting method) is described Fig. 1.

2. Method

In this section, the data preprocessing method, optimization method, basic forecasting method and proposed forecasting system are described.

2.1. Data preprocessing module: Ensemble empirical mode decomposition

For data preprocessing, ensemble empirical mode decomposition is used in this paper proposed by Wu and Wang in 2008. This method improved traditional empirical mode decomposition in order to overcome the imperfection of mode mixing [35]. Empirical mode decomposition, proposed by Huang in 1998, was designed to divide the nonstationary signals into several intrinsic mode function [36]. The intrinsic mode functions must simultaneously satisfy two conditions: (1) Across the entire time range, the number of local extreme points and zero-crossing points must be equal, or the maximum difference should be 1. (2) At any time point, the average value of the envelope (upper envelope) of the local maximum value and the envelope (lower envelope) of the local minimum must be zero [37].

Ensemble empirical mode decomposition was developed based on traditional empirical mode decomposition. This decomposition method adds Gaussian white noise to the initial sequence before decomposing the signal. Mode mixing problems that occur after empirical mode decomposition can be improved by adding Gaussian noise, and then sequence added Gaussian white noise can be further applied to process and decompose complex nonstationary signals. A nonlinear and nonstationary complex signal is decomposed into a series of orthogonal and complete intrinsic mode functions with different characteristic scales and a residual function [38].

According to the above description of ensemble empirical mode decomposition, the basic idea of this method is as follows [39]:

Step 1: Add a white-noise series with normal distribution to the original signal.
Step 2: Decompose the signal, which is preprocessed, and obtain several intrinsic mode functions.
Step 3: Repeat the above steps, with new white noise added each time.
Step 4: The ensemble means of the decomposition results over *N* times is regarded as the final decomposition result.

Ensemble empirical mode decomposition is a great improvement over the traditional empirical mode decomposition method, effectively solving the frequency mode mixing problem of traditional empirical mode decomposition and preserving the authenticity of the signal to a great extent [39].

2.2. Optimal module: Multi-objective differential evolution

To optimize the weight in the amended equation and the interval length of the FTS algorithm, a novel optimal algorithm called the Multi-Objective Differential Evolution (MODE), which consists of multi-objective optimization and standard Differential Evolution (DE), is developed in forecasting system.

2.2.1. Differential evolution

The DE algorithm was proposed by Storn and Price in 1995, and became a popular evolutionary algorithm in solving the problem of continuous global optimization because of its robustness and speed [40]. Compared to a simple GA, DE obtained a more exact optimum value with less generation [41].

Like GA, the DE algorithm is an optimization algorithm based on modern intelligence theory, and guides the direction of the optimization search based on the swarm intelligence generated by cooperation and competition between individuals [42]. DE has a wide application owing to its advantages of simple structure, simple operation, and robustness [43].

A differential evolution algorithm is an effective and parallel direct-search evolutionary algorithm. Assume that a population contains *NP* individuals and the dimension of the solution is *D*, then the *i*th individual can be represented by a vector.

$$\vec{x}_{i,G} = \{x_{1,i,G}, x_{2,i,G}, \cdots, x_{D,i,G}\}, \quad i = 1, 2, 3, \ldots, NP \tag{1}$$

where *D* denotes the dimension of the problem, and the initial population ($G = 0$) is supposed to randomly distribute between the prescribed upper bound and lower bound $[\vec{x}_{\min}, \vec{x}_{\max}]$. A more detailed basic strategy for the differential evolution algorithm is discussed below [44].

Mutation operation

The aim of a mutation operation is to use a random element to produce a variation vector, and then make the population change in a good direction. This algorithm generates a variation vector $\vec{v}_{i,G}$ for each target vector $\vec{x}_{i,G}$ by a deterministic mutation strategy. The mutation strategy applied in this paper is

$$\vec{v}_{i,G} = \vec{x}_{r_1,G} + F\cdot(\vec{x}_{r_2,G} - \vec{x}_{r_3,G}) \tag{2}$$

where r_1, r_2, and r_3 are randomly selected from {1, 2, 3,…, NP}, are mutually different integers, and are different from the running index i. F is a scaling factor and positive real number that is between 0 and 2. It controls the amplification of differential variation $(\vec{x}_{r_2,G} - \vec{x}_{r_3,G})$.

Crossover operation

After the mutation operation, to enhance the potential diversity of the population, a crossover in the DE algorithm is introduced to form a trial vector:

$$u_{i,G} = (u_{1i,G}, u_{2i,G}, \cdots, u_{Di,G})$$

where

$$u_{ji,G} = \begin{cases} v_{ji,G} & if\,(randb(j) \leqslant CR)\ or\ j = rnbr(i) \\ x_{ji,G} & if\,(randb(j) > CR)\ and\ j \neq rnbr(i) \end{cases}, \quad j = 1, 2, ..., D. \tag{3}$$

where $randb$ (j) is the jth evaluation of a uniform random number generation with an outcome between 0 and 1. CR is a random integer called the crossover constant between 0 and 1, and is applied to control the replicating content of a mutant individual by population individuals. $rnbr(i)$ is a random integer between 1 and D that ensures at least one value for the dimension of $u_{i,G}$ is derived from the variation vector $v_{i,G}$.

Selection operation

After the trial vector $u_{i,G}$ is obtained, $f(\vec{x}_{i,G})$ and $f(\vec{u}_{i,G})$ are calculated, and $f(\vec{x})$ is the objective function of optimization. A greedy criterion was applied in DE algorithm to keep the individuals who obtained better solutions in the next generation.

$$\vec{x}_{i,G+1} = \begin{cases} \vec{u}_{i,G}, & if\ \ f(\vec{u}_{i,G}) \leqslant f(\vec{x}_{i,G}) \\ \vec{x}_{i,G}, & otherwise \end{cases} \tag{4}$$

2.2.2. Multi-objective differential evolution

In this paper, Multi-objective Differential Evolution is realized by a weighing factor method. This method combines several different objectives into a single objective by multiplying each objective by a defined weight. The classical and simplest multi-objective strategies are most widely applied. The value of the weight for an objective is given according to the relative importance of the objective for specific issues.

Then, a composite objective function can be formed by summing the weighted objective, and the multi-objective optimization problem is converted into a single-objective optimization issue. Moreover, the sum of the weighs is 1 in usual practice [45]. The multi-objective problem in our paper can be stated as follows:

$$Objectives \begin{cases} \mathbf{o_1}: \min f_1 = RMSE(y, \hat{y}) \\ \mathbf{o_2}: \min f_2 = std(error) \end{cases} \tag{5}$$

$$RMSE = \sqrt{\frac{1}{N} \times \sum_{i=1}^{N} (y_i - \hat{y}_i)^2} \tag{6}$$

$$std = \sqrt{E(\hat{y} - E(\hat{y}))^2} \tag{7}$$

where N is the number of observations, y_i is the actual values, and $\hat{y}_i$ is the forecasting values.

The main goal of our paper is to make both of the objectives (o_i) a minimum. To realize this simply, the weighing factor method is applied in our paper to sum the two objectives into a single objective:

$$O = \sum_{i=1}^{m} w_i o_i, \quad \sum_{i=1}^{m} w_i = 1, \quad w_i > 0 \tag{8}$$

where m is the number of objectives, and w_i is the weights of each objective, which is nonnegative and less than 1.

2.3. Forecasting module: Fuzzy time series (FTS) algorithm

In the proposed forecasting system, fuzzy time series is applied as the basic method. The concept of a fuzzy set was derived in the last century and proposed by Zadeh [46]. The concept of a fuzzy time series (FTS) was defined by Song and Chissom [47] and was first proposed for college enrollment forecasting [48]. FTS has been frequently and successfully applied in several fields owing to its easy calculations and accurate forecasting via handling linguistic value datasets [49].

The definitions of FTS are as follows:

Definition 1. $Y(t)(t = 0, 1, 2, ...)$ is a series of raw data, regarded as the universe of discourse. The fuzzy sets $f_j(t)$ are obtained on this basis. The fuzzy time series F(t), defined on Y(t), consists of $f_1(t)$, $f_2(t)$, ….

Definition 2. In the FTS relationship, it is assumed that F(t) is influenced only by F(t − 1). Then, the forecasting model can be expressed as F(t) = F(t − 1) × R(t − 1, t). F(t) is the fuzzy set at time t, F(t − 1) is the fuzzy set of the previous moment, and R (t − 1, t) represents the fuzzy logical relationship (FLR).

Definition 3. Set F(t − 1) = A_i and F(t) = A_j. Their FLR can be described as $A_i \rightarrow A_j$, in which A_i and A_j are, respectively, the left-hand side (LHS) and right-hand side (RHS) of the FLR. Then, all the single FLRs can be composed into different groups on the basis of the same LHS.

2.4. Proposed forecasting system

In our study, fuzzy time series is selected as the basic model to perform forecasting of wind speed. However, the different intervals partition and weight of amended equation in FTS would have a significant influence on the accuracy of forecasting results, so it is crucial to determined optimal interval cut points and weight to improve the forecasting performance. MODE is developed to optimize the cut points and weight. Furthermore, the original wind speed sequences are full of noise, which could have a negative impact on forecasting effects. So, Ensemble empirical mode decomposition is applied to eliminate the noise pollution from the original time series.

The steps of the hybrid forecasting system are described as follows:

Step 1: Data pre-processing technique based on decomposition and ensemble strategy introduced in Section 2.1 is applied to eliminate the noise and decrease the uncertainty of the original data.
Step 2: Take both accuracy and stability into account, multi-objective differential evolution introduced in Section 2.2 is used to optimize the interval cut points and weight of the fuzzy time series.
Step 3: Define $\boldsymbol{U}$ = [min − d_1, max + d_2] as the universe of discourse. Then, partition it into several adjoining intervals based on optimal cut points obtained by MODE. The continuous observational values can be assigned to corresponding linguistic values.
Step 4: Determine the fuzzy membership function to define the fuzzy set for the raw observational values. Then, fuzzy set A_i is constructed on the basis of intervals [50]:

$$A_i = \frac{f_{A_i}(u_1)}{u_1} + \frac{f_{A_i}(u_2)}{u_2} + \cdots + \frac{f_{A_i}(u_j)}{u_j} + \cdots + \frac{f_{A_i}(u_n)}{u_n} \tag{9}$$

where f_{A_i} denotes the membership function of A_i and $f_{A_i}(u_j)$ is the grade of membership of u_j in A_i. The value of $f_{A_i}(u_j)$ can be defined as follows [51]:

$$f_{A_i}(u_j) = \begin{cases} 1\,, & i = j \\ 0.5\,, & i = j+1 \\ 0\,, & others \end{cases} \tag{10}$$

Step 5: The actual values are then fuzzified. An original value is fuzzified to A_i when the highest degree of membership of that

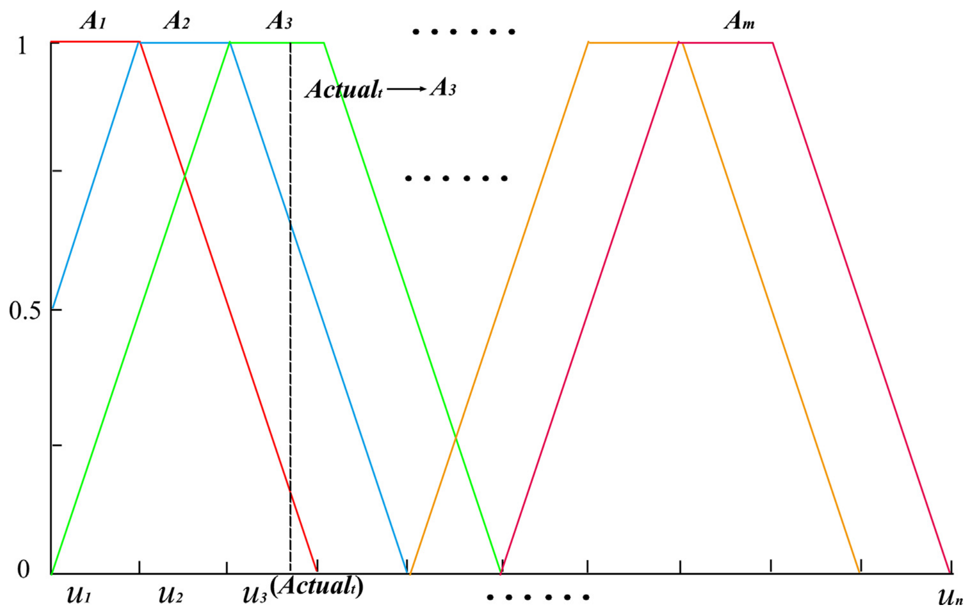

Fig. 2. Membership functions and fuzzification process for fuzzy time series.

original value is in A_i [52].

$$\textbf{\textit{fuzzify}}(actual_t) = A_i \quad if \quad f_{actual_t}(A_i) = \mathbf{max}[f_{actual_t}(A_z)] \quad z = 1, 2, 3, \ldots m \tag{11}$$

where m is the number of the fuzzy set and $f_{actual_t}(A_z)$ is the degree of membership of actual value at t under A_z. The clearer expression can be described as Fig. 2.

Step 6: Establish and group the FLR. For instance, $\boldsymbol{A_i \rightarrow A_j}$,$\boldsymbol{A_i \rightarrow A_k}$,$\boldsymbol{A_i \rightarrow A_l}$ can be grouped into $\boldsymbol{A_i \rightarrow A_j, A_k, A_l}$.

$$\left.\begin{array}{l} t = m,\, A_i \rightarrow A_j \quad with\ weight\ 1 \\ t = n,\, A_i \rightarrow A_k \quad with\ weight\ 1 \\ t = p,\, A_i \rightarrow A_l \quad with\ weight\ 1 \end{array}\right\} \Rightarrow A_i \rightarrow A_j,\, A_k,\, A_l$$

Step 7: Calculate weights. Based on step 6, the weight matrix can be determined and further standardized. Then, the centroid defuzzification method is applied to calculate the defuzzification matrix.

$$\boldsymbol{W\_s}(t) = (\widehat{W}_1, \widehat{W}_2, \cdots, \widehat{W}_k) \qquad \widehat{W}_i = W_i / \sum_{i=1}^{k} W_i \tag{12}$$

$\boldsymbol{W\_s}$ denotes the standardized weighting matrix, $\boldsymbol{W_i}$ is the weighting matrix elements that are unstandardized, and $\boldsymbol{\hat{W}_i}$ represents standardized ones.

Step 8: Obtain the forecasting results. The rudimentary forecasting results can be obtained by multiplying the defuzzified matrix by standardized weighting matrices, which can be expressed as follows:

$$\boldsymbol{F}(t) = \boldsymbol{D}(t-1) \times \boldsymbol{W\_s}(t-1) \tag{13}$$

Here, F (t) represents the forecasting result, $\boldsymbol{D}$ represents the defuzzified matrix.

Step 9: Finally, the forecasted results obtained in step 8 are amended by applying Eq. (14) to determine the ultimate forecasting results. And the optimal weight α is searched by MODE.

$$\boldsymbol{F\_u}(t) = y(t-1) + \alpha \times (\boldsymbol{F}(t) - y(t-1)) \tag{14}$$

where $y(t-1)$ denotes the raw value at time $t-1$, and $\boldsymbol{F\_u}$ denotes the final forecasting results at time t. α is the weight for amending the forecasting results which will be optimized by MODE.

According to the above process, the universes of discourse for wind data at three sites are determined as (2, 18.5), (2, 17), and (2, 18.5), respectively, and the number of the intervals is set to 10. Thus, the number of decision variables that need to be optimized is 10, namely, the dimension of the problem to solve is 10, including nine cut points and the weight in the mend equation. Through repeated experiments, the parameters of MODE in this study are shown in Table 1. The partition results according to MODE algorithm of the three sites are presented in Table 2. In Table 2, u1-u10 is the 10 intervals determined according to cut points which are determined by multi-objective differential evolution algorithm. For example, the 10 intervals for wind speed time series in site 1 are respectively (2.0, 3.5), (3.5, 5.2), (5.2, 6.3), (6.3, 7.0), (7.0, 8.1), (8.1, 9.7), (9.7, 11.1), (11.1, 12.6), (12.6, 14.2), and (14.2, 18.5).

3. Experiments and analysis

To compare the performance of the proposed hybrid forecasting system and other models, several experiments are performed. In this section, the experimental results and related analysis will be presented.

3.1. Data description

Shandong province is located on the eastern coast of China and along the lower Yellow River. The province has a long coastline. Shandong possesses hundreds of coastal islands with high wind power density and high average annual wind speed, and is one of the wind-energy-rich regions in China. In recent years, in order to promote

Table 1
Experimental parameters of MODE algorithm.

Parameter	Setting
Number of objectives	2
Number of decision variables (**D**imension)	10
Population size (***NP***)	100
Maximum number of iterations	1000
crossover constant	0.8
mutation rates	0.6
number of initialization generation	1
Min limit Minimum value of the universe of discourse	
Max limit Maximum value of the universe of discourse	

Table 2
Interval partition results for three sites by MODE.

Sites	Site1	Site2	Site3
u_1	(2.0, 3.5)	(2.0, 3.8)	(2.0, 4.4)
u_2	(3.5, 5.2)	(3.8, 5.0)	(4.4, 5.7)
u_3	(5.2, 6.3)	(5.0, 6.1)	(5.7, 6.6)
u_4	(6.3, 7.0)	(6.1, 7.1)	(6.6, 7.4)
u_5	(7.0, 8.1)	(7.1, 7.8)	(7.4, 8.6)
u_6	(8.1, 9.7)	(7.8, 9.0)	(8.6, 9.9)
u_7	(9.7, 11.1)	(9.0, 10.5)	(9.9, 11.5)
u_8	(11.1, 12.6)	(10.5, 12.1)	(11.5, 13.0)
u_9	(12.6, 14.2)	(12.1, 13.7)	(13.0, 14.6)
u_{10}	(14.2, 18.5)	(13.7, 17.0)	(14.6, 18.5)

energy conservation, emission reduction, and environmental protection, large-scale wind farms in coastal areas have been established in Shandong such as Weihai, Yantai, and Qingdao, and gradually developed offshore wind power projects.

By the end of June 2017, there were 42 grid-connected wind farms in the Yantai power grid, with 1607 wind turbines and 2.53 million kw of wind power installed capacity. This accounts for 27.9% of the total installed capacity of wind power in Shandong province. From the national wind energy resource distribution map, it can be seen that Penglai has a unique geographical location and natural conditions for the development and utilization of wind energy [53].

Penglai belongs to Yantai and is located at the northern end of the Shandong Peninsula at 120°40′E–120°445′E and 37°40′N–37°47′N and the zone of the continental monsoon climate. It is one of the most dynamic regions in China's Bohai Sea Economic Zone and a low-mountain and hilly landform that is low in the south and high in the north. According to the data of wind measurement mast, the average wind speed and wind power density at a height of 70 m are 6.05 m/s and 235.54 W/m^2 which are 5.72 m/s and 201.27 W/m^2 at a height of 50 m, 5.26 m/s and 157.07 W/m^2 at a height of 30 m. Based on the wind power density scale, the wind power density in this wind farm has reached the 2-level wind condition standard and wind resources are rich which can be used to generate electricity.

Therefore, it is vital to forecast the wind speed accurately in this area. Accordingly, the short-term wind speed data of WTG10, WTG 28 and WTG 35 from local wind farms in Penglai are used to demonstrate the forecasting effectiveness of the proposed hybrid forecasting system. The samples are taken at 10-min intervals and a 144-times-per-day sampling frequency, recorded from 0:00 on 1 January 2011 to 23:50 on 20 January 2011. For each site, the number of data selected in this paper are 2880, and 2000 of which are used as the input for training to establish the weight matrix for the model and the rest for testing. The selected area, line chart and boxplot of the three datasets are visualized in Fig. 3. Additionally, several statistical indicators such as mean of wind speed data including all samples, training sets and testing sets at the three sites are listed in Table 3.

3.2. Evaluation metrics

In order to comprehensively evaluate the forecast results, several evaluation metrics are selected to compare the performance of the competitive models from three aspects: accuracy, stability, and direction. The mean absolute error (MAE), root mean square error (RMSE), mean absolute percentage error (MAPE), and Theil inequality coefficient (TIC) (which is calculated based on forecasting errors) are used to evaluate the forecasting accuracy. Compared to the mean error, MAE can better reflect the forecasting error because the absolute value of deviation is used to calculate and avoid the canceling effect of the positive and negative values. RMSE is sensitive to extra-large or small values, so it can better measure the precision of the values. For stability, the variance (VAR) of the forecasting error is applied to evaluate the stability of the forecasting models. With respect to direction, the direction accuracy (**DA**) of the forecasting results is used to calculate the correctness of the forecasted direction. The specific definition and calculating equation of evaluation metrics are presented in Table 4.

3.3. ***Experiment I:*** *Comparison between different partition methods (MODE, equal width, and equal frequency)*

As we know, in a fuzzy time series method, the discretization method is an important factor in the forecasting performance. Equal Width (EW) and Equal Frequency (EF) interval algorithms are the simplest and most common unsupervised discretization methods, but satisfactory results cannot always be achieved by them.

Thus, in our proposed forecasting system, the MODE algorithm is applied to search the optimal cut points in a fuzzy time series. The performance of the fuzzy time series are compared in Experiment I when the intervals are partitioned by different methods to verify the effectiveness of the MODE algorithm.

By taking site I as an example, the forecasting results and errors are depicted in Fig. 4. The purple curve of the forecasting value in our proposed forecasting system is closer to the pink bar graph of the actual value. The improvement ratios generated by MODE are about 15% compared with the fuzzy time series method under equal widths and equal frequency methods. The forecasting error between the forecasting value and actual value also demonstrates that the error in our proposed system is concentrated more around the zero-scale line, and the volatility of the error is the least, followed by the equal width interval discretization method. Moreover, it can be clearly seen that the forecasting performance is better when the fluctuation of the wind speed time series is relatively small.

According to the evaluation metrics described in Section 3.2, the forecasting performance of the different models is presented in Table 5, and the best value is marked in bold. As for accuracy, taking MAPE as an example, the values of the proposed forecasting system are, respectively, 3.8395%, 3.6180%, and 3.5478% for the three sites. These are evidently lower than the other two methods with the MAPE above 4% and some even close to 5%. On the whole, the MAPE value of the equal width interval discretization method is lower than that of the equal frequency method. The stability evaluation indicator, which is the variance of the error, shows that the stability of the proposed forecasting system is superior to the other two methods, among which the equal width interval discretization method is superior to the equal frequency method. It can be seen from the direction accuracy indicator that very little difference exists between the equal width and equal frequency method, but our proposed system is more accurate than these two methods.

Remark 1. The interval partition plays a vital role in the performance fuzzy time series method. Thus, it makes sense to search an optimal discretization method. From our experiment, it can be concluded that the accuracy of our proposed forecasting system is better than that of the fuzzy time series model with the EW and EF interval discretization methods. In addition, the stability and future change forecasting of our system are outstanding. In terms of the two compared models, the forecasting effectiveness of the equal width interval discretization method is better than that of the equal frequency method in all three aspects. In all, the MODE algorithm can search relatively better cut points for fuzzy time series, and can further achieve a better performance in accuracy, stability, and future change forecasting.

3.4. ***Experiment II:*** *Comparison between multi-objective differential evolution and other optimization algorithms*

The purpose of Experiment II is to compare different optimization algorithms applied to weight fuzzy time series. Four well-known optimization algorithms [Particle Swarm Optimization (PSO), Cuckoo

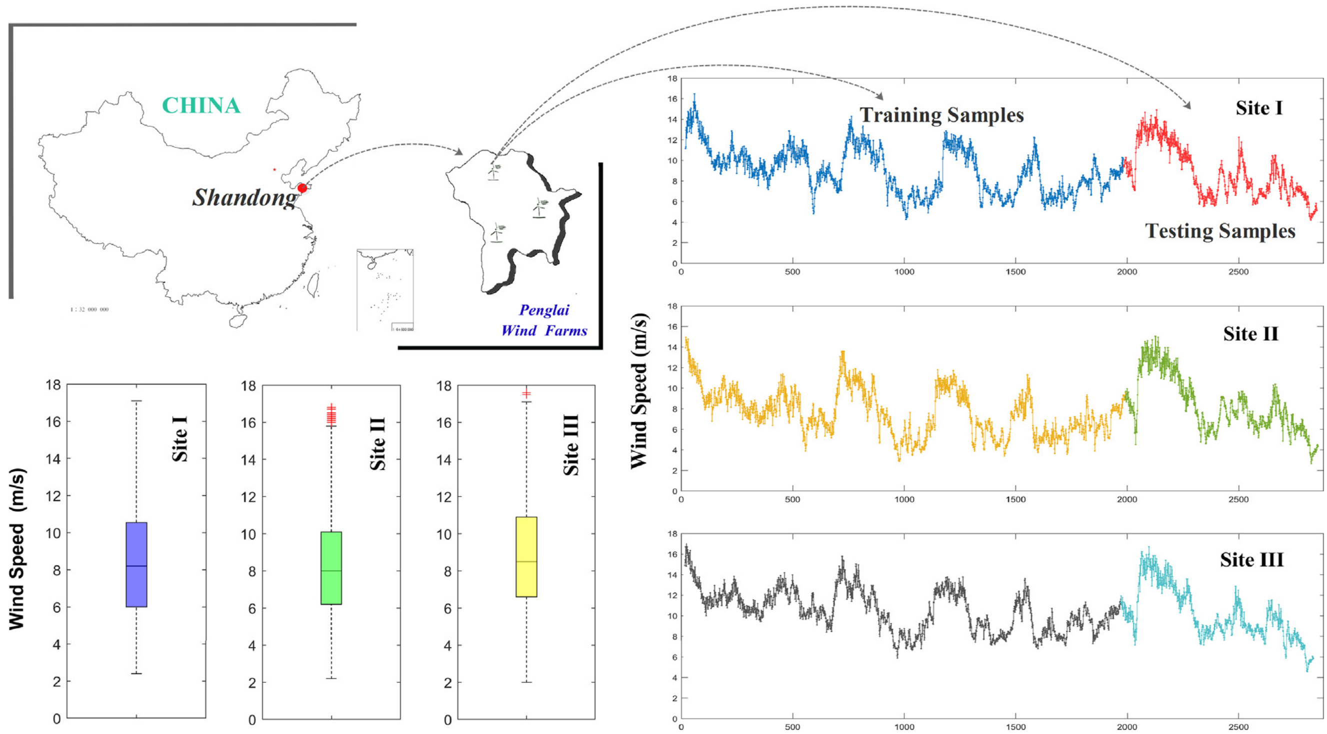

Fig. 3. Description of wind speed time series at three sites.

Search (CS), Harmony Search (HS), and Firefly Algorithm (FA)] are selected to compare with Multi-Objective Differential Evolution (MODE) to search the optimal cut points and weight in mend equation. The parameters determined by the algorithms in this paper are obtained on the basis of analyses from our experiments and literature, which are presented in Table 6.

Comparison between different optimal algorithms is showed in Table 7. It can be found that a lowest value for the MAE, RMSE, MAPE, and TIC is achieved by MODE algorithm. This verifies the stability of the forecasting results for all three sites. The nearly same accuracy is obtained by CS and HS at site I, and the poorest accuracy is achieved by CS at site II, while HS is the worst at site III. In terms of future change forecasting, the best DA is obtained by PSO at sites I and II, while MODE is the best at site III. However, MODE outperforms the other algorithms in forecasting stability for all three sites. Concretely, the MAPE of MODE is about 0.25% lower than those of CS and HS, and the variance of the error is about 0.03 lower than CS.

Remark 2. Combining indicators of all three aspects, the best performance in forecasting accuracy and stability is presented by MODE algorithm, which focuses on optimizing both the forecasting accuracy and stability, and future changes in wind speed time series can be more accurately caught by PSO. The CS and HS algorithms perform the most poorly among all five optimization algorithms.

3.5. *Experiment III: Comparison between our proposed system and other models*

Experiment III is designed to compare the performance of our proposed forecasting system with some widely applied statistical forecasting models, artificial neural networks, and other well-known models. The forecasting and evaluation results are presented in Fig. 5 and Table 9.

Among the numerous ANNs, three popular models are selected: the

Table 3
Statistical indicators of wind speed data at three sites.

Datasets	Statistical indicators					
	Maximum (m/s)	Minimum (m/s)	Median (m/s)	Mean (m/s)	Interquartile range (m/s)	Std. (m/s)
Equation	–	–	–	$\textit{Mean} = \sum_{i=1}^{N} x_i / N$	$Q_d = Q_U - Q_L$	$S = \sqrt{\frac{1}{N}\sum_{i=1}^{N}(x_i - \bar{x})^2}$
Site I						
All samples	18.1	2.4	8.2	8.4413	4.55	2.9139
Training set	18.1	2.5	8.4	8.5090	4.30	2.8054
Testing set	16.1	2.4	7.5	8.2874	4.85	3.1430
Site II						
All samples	16.8	2.2	8.0	8.3167	3.90	2.8354
Training set	16.7	2.5	7.9	8.0744	4.00	2.6398
Testing set	16.8	2.2	8.2	8.8673	4.15	3.1697
Site III						
All samples	18.4	2.0	8.5	8.7969	4.30	2.9919
Training set	18.4	2.0	8.6	8.6368	4.50	2.8735
Testing set	17.6	2.1	8.4	9.1608	4.35	3.2173

Table 4
Specific definitions of evaluation metrics.

Metric	Definition	Equation
MAE	Mean absolute error of forecasting results	$\mathbf{MAE} = \frac{1}{N}\sum_{i=1}^{N}\lvert y_i - \hat{y}_i\rvert$
RMSE	Root mean square value of the errors	$\mathbf{RMSE} = \sqrt{\frac{1}{N} \times \sum_{i=1}^{N}(y_i - \hat{y}_i)^2}$
MAPE	Average of absolute percentage error	$\mathbf{MAPE} = \frac{1}{N}\sum_{i=1}^{N}\left\lvert\frac{y_i - \hat{y}_i}{y_i}\right\rvert \times 100\%$
TIC	Theil inequality coefficient of forecasting results	$\mathbf{TIC} = \sqrt{\frac{1}{N}\sum_{i=1}^{N}(y_i - \hat{y}_i)^2} / \left(\sqrt{\frac{1}{N} \times \sum_{i=1}^{N} y_i^2} + \sqrt{\frac{1}{N} \times \sum_{i=1}^{N} \hat{y}_i^2}\right)$
VAR	Variance of the forecasting error	$\mathbf{Var} = E(\hat{y} - E(\hat{y}))^2$
DA	Direction accuracy of forecasting results	$\mathbf{DA} = \frac{1}{l}\sum_{i=1}^{l} w_i,\ w_i = \begin{cases} 1, & if\ (y_{i+1} - y_i)(\hat{y}_{i+1} - y_i) > 0 \\ 0, & otherwise \end{cases}$

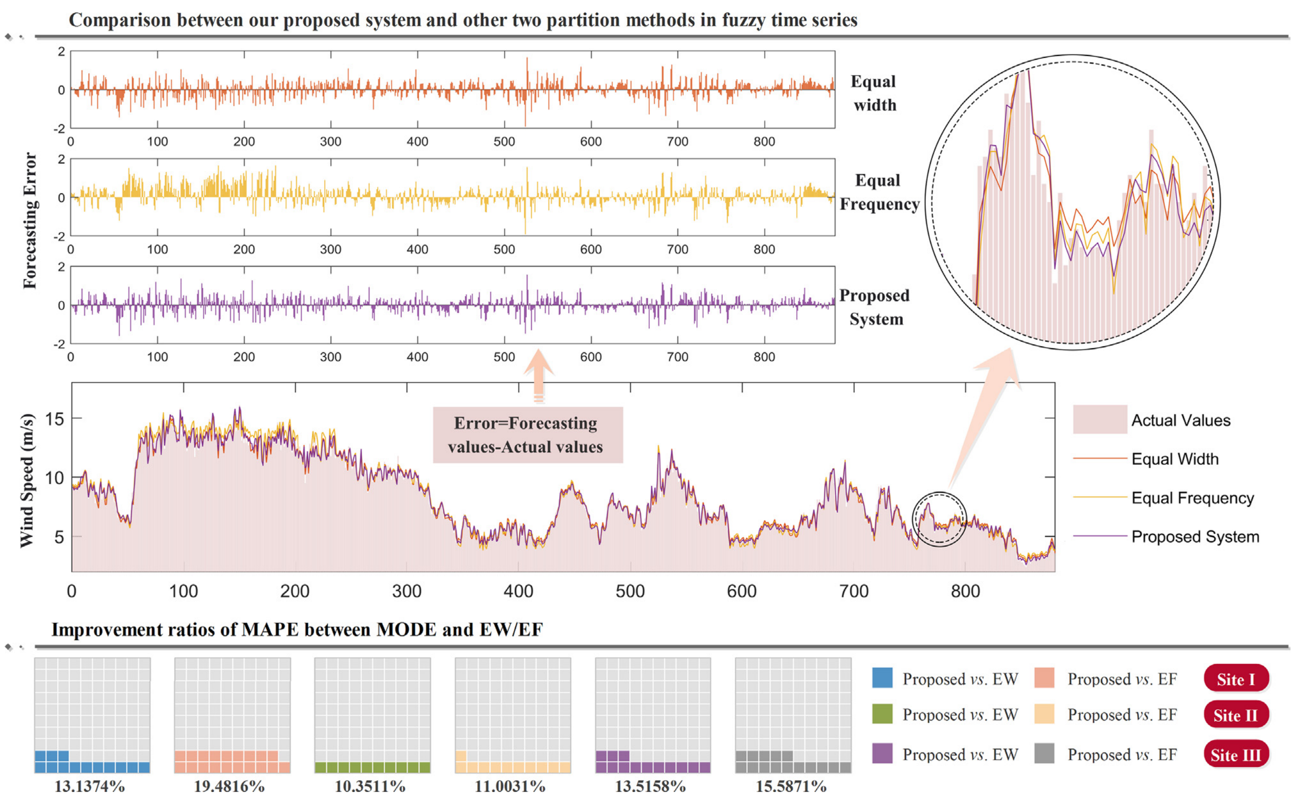

Fig. 4. Forecasting results of fuzzy time series under different partition methods.

Back Propagation Neural Network (BPNN), Extreme Learning Machine (ELM), and Elman neural network. Then, the two most widely used statistical models, Auto-Regressive Integrated Moving Average (ARIMA) and Double Exponential Smoothing (DES), are established for comparison. Apart from these two methods, Support Vector Regression (SVR) is applied in the comparison experiments of our paper owing to its unique merits in solving small samples and nonlinear and high-dimensional pattern recognition. For the ANN, the number of input and output layers is set to 5 and 1, respectively. The hidden layers in BPNN, ELM, and Elman are selected as 2, 20, and 25. The structure of training and testing sets of ANN is presented in Fig. 5. In the ARIMA (p, d, q) model, $p = 7$, $d = 1$, and $q = 9$ that are set based on the A-Information

Table 5
Forecasting results of fuzzy time series under different partition methods.

	Methods	MAE	RMSE	MAPE (%)	TIC	DA	VAR
Site I	*EEMD-EW-FTS*	0.333524	0.423226	4.420214	0.023886	0.730375	0.179235
	EEMD-EF-FTS	0.367900	0.483104	4.768490	0.027030	0.703072	0.223203
	EEMD-MODE-FTS	**0.298760**	**0.397983**	**3.839513**	**0.022445**	**0.750853**	**0.158524**
Site II	*EEMD-EW-FTS*	0.336820	0.432852	4.035736	0.023012	0.756542	0.187527
	EEMD-EF-FTS	0.343217	0.453161	4.065308	0.024084	0.750853	0.205588
	EEMD-MODE-FTS	**0.305595**	**0.400672**	**3.617997**	**0.021281**	**0.773606**	**0.160705**
Site III	*EEMD-EW-FTS*	0.342054	0.433321	4.102275	0.022353	0.736064	0.187796
	EEMD-EF-FTS	0.364843	0.479188	4.202937	0.024641	0.739477	0.228615
	EEMD-MODE-FTS	**0.304329**	**0.404509**	**3.547821**	**0.020822**	**0.787258**	**0.163669**

Table 6
Experimental parameter values in different optimization algorithms.

Methods	Parameters	Value
PSO	Evolution generations	1000
	Population size	100
	Maximum velocity	1
	Minimum velocity	−1
CS	Discovery rate of alien eggs/solutions	0.25
	Tolerance	0.001
	Total number of iterations	1000
HS	Maximum Number of Iterations	1000
	Harmony Memory Size	1
	Number of New Harmonies	1
	Harmony Memory Consideration Rate	0.95
	Pitch Adjustment Rate	0.25
FA	Maximum Number of Iterations	100
	Number of Fireflies (Swarm Size)	100
	Light Absorption Coefficient	0.6
	Attraction Coefficient Base Value	0.08
	Mutation Coefficient	0.4
	Mutation Coefficient Damping Ratio	0.98

Table 7
Forecasting results of fuzzy time series under different optimization algorithms.

Indicators	EEMD-PSO-WFTS	EEMD-CS-WFTS	EEMD-HS-WFTS	EEMD-FA-WFTS	EEMD-MODE-WFTS
Site I	*Different optimization algorithms*				
MAE	0.309215	0.321744	0.317249	0.308160	0.298760
RMSE	0.409583	0.428939	0.421072	0.413061	0.397983
MAPE (%)	3.939860	4.072999	4.079950	3.953990	3.839513
TIC	0.023105	0.024196	0.023747	0.023303	0.022445
DA	0.759954	0.745165	0.742890	0.740614	0.750853
VAR	0.167893	0.184162	0.177167	0.170763	0.158524
Site II	*Different optimization algorithms*				
MAE	0.318162	0.329822	0.313062	0.320367	0.305595
RMSE	0.425606	0.435247	0.415790	0.426078	0.400672
MAPE (%)	3.777478	3.918208	3.723828	3.745084	3.617997
TIC	0.022628	0.023109	0.022081	0.022650	0.021281
DA	0.778157	0.761092	0.772469	0.765643	0.773606
VAR	0.181137	0.189402	0.172950	0.181661	0.160705
Site III	*Different optimization algorithms*				
MAE	0.312433	0.327559	0.329091	0.317451	0.304329
RMSE	0.418322	0.442193	0.443374	0.433233	0.404509
MAPE (%)	3.627804	3.754795	3.795713	3.591513	3.547821
TIC	0.021527	0.022776	0.022847	0.022287	0.020822
DA	0.782708	0.766780	0.770193	0.770193	0.787258
VAR	0.174932	0.195757	0.196802	0.187326	0.163669

Criterion (AIC) and a stability test [54]. For the SVR model, the radial basis function is chosen as a kernel function, which is the key to SVR. The detailed parameters of the competitive models, such as learning rate and iteration times, are presented in Table 8, and other parameters are at their default settings.

Then, the comparison results are analyzed as follows:

(1) Considering all the three sites, our proposed hybrid forecasting system has the best performance. The forecasting accuracy of our proposed system at site I with a MAPE of 3.84% is much better than those of the other models. Our proposed hybrid forecasting system's variance of error, which evaluates the forecasting stability, is also the best. It is also shown in Fig. 5 that the proposed system's scatter plot of forecasting and actual values is closest to the diagonal, which indicates that the difference between the forecasting value and actual value is the smallest.
(2) As shown in Table 9, the poorest forecasting performance is presented by the Elman neural network among the ANNs in accuracy, stability, and future change forecasting, while better performance is achieved by ELM. For the statistical model, the forecasting accuracy of DES is the lowest with a MAPE of 5% higher than that of our proposed hybrid forecasting system. The variances of the DES method's forecasting error are all higher than 1, while the proposed system's variance is about 0.16. This can verify the good stability of our proposed hybrid forecasting system.
(3) When conventional statistical models are applied to some practical forecasting processes, the former always have poor extrapolation performance and a narrow forecasting scale owing to their inherent nonlinearity and instability. For artificial neural networks, the forecasting results are usually unstable and have a high dependence on data. Moreover, there is no unified setting standard for parameters in these artificial neural network models, which significantly influences the forecasting results.
(4) The persistence model, a popular and widely used benchmark model, regards the actual value at time $t - i$ as the forecasting value at time t. i is the forecasting step, which is set as 1 in our paper. As a standard, this model is adopted to measure the performance of our proposed system. The compared results are presented Table 9 in detail. Because the forecasted value at t is equal to the last observation, the value of DA is always 0 for this model, which is meaningless. Regarding the other two aspects, accuracy and stability, our proposed hybrid system obtains better results for all metrics.

Remark 3. Compared with the other models, the forecasting accuracy, stability, and other performance factors can be significantly improved by our proposed hybrid forecasting system. Among other competitive models and the benchmark persistence model, the Elman neural network and DES method possess relatively poor performance.

3.6. ***Experiment IV:*** *Comparison between single-objective and multi-objective methods*

In order to compare the forecasting effectiveness of the multi-objective optimization method, a single-objective optimization algorithm [a differential evolution (DE) algorithm that regards the forecasting accuracy as the only optimization goal] is applied to forecast the same wind speed time series. The results are presented in Table 10. It can be observe that for the accuracy indicator, the value of MAPE at site III obtained by the single-objective optimization algorithm is lower than that of multi-objective optimization, but for the other indicators at three sites, multi-objective optimization all outperforms the single-objective optimization algorithm. For stability and forecasting change forecasting, the fuzzy time series methods tuned by MODE algorithm are all superior to that of the fuzzy time series method tuned by DE on the whole for the three sites.

Remark 4. Most common optimization algorithms can focus only on one objective, but in the meantime, other objectives also vital for forecasting are always neglected. Thus, to remedy the limitations of single-objective optimization, MODE with two objectives, forecasting accuracy and stability, shows greater performance than the differential evolution method.

4. Discussion

In this section, in order to further verify the effectiveness of our proposed hybrid forecasting system, the forecasting results at different time intervals of wind speed data are discussed in our study. Moreover, the DM, forecasting effectiveness, and Grey relation of the different models are discussed to analyze the forecasting performance from different aspects.

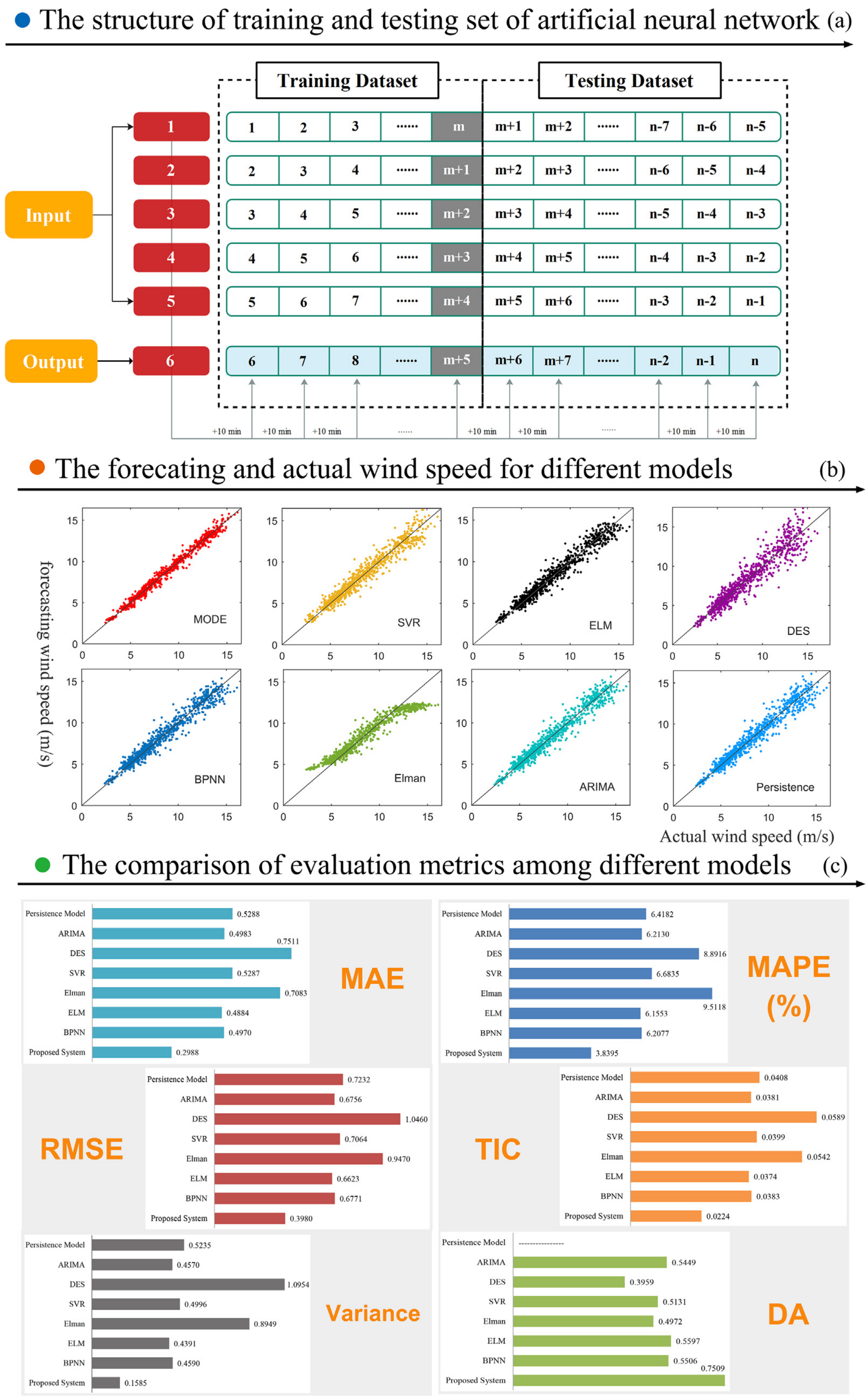

Fig. 5. Comparison results of our proposed system with other competitive models.

4.1. Forecasting results at different time intervals of wind speed data

As we all know, in actual, economically productive activities, the focal points and time intervals of wind speed time series examined by different managers are diverse [55]. In the electricity market and real-time operations, ultra-short-term wind speed data is required. For reserve requirement decisions and generator online/offline decisions, medium-term wind speed data is more suitable. When the optimal

Table 8
Experimental parameter settings in different models.

Model	Experimental parameter	Value
BPNN	Maximum number of iteration times	1000
	Learning rate	0.01
	Training accuracy goal	0.00001
	Node-point number of input layer	5
	Node-point number of hidden layer	2
	Node-point number of output layer	1
ELM	Node-point number of input layer	5
	Node-point number of hidden layer	20
	Node-point number of output layer	1
Elman	Node-point number of input layer	5
	Node-point number of hidden layer	25
	Node-point number of output layer	1
	Iteration number of display once in an image	20
	Maximum number of iteration times	1000
SVR	Node-point number of input layer	5
	Node-point number of output layer	1
	Type of SVR model	epsilon-SVR
	Type of kernel function	RBF
	Parameter of epsilon-SVR	4
ARIMA (*p, d, q*)	Autoregressive term (*p*)	7
	Moving average number (*q*)	9
	Difference times (*d*)	1
DES	Smoothing coefficient	0.9

operating costs and maintenance planning need to be formulated, long-term wind speed data is always essential. The main wind speed forecasting horizons with their respective utilities for different sectors are presented in Table 11.

Thus, to meet various requirements in practical applications and to prove the practicality of our proposed hybrid system, data for two other time intervals of wind speed (30 min and 60 min) are collected. The six evaluation metric results for eight different models are presented in Table 12: the proposed hybrid system, BP, Elman, ELM, SVR, DES, and ARIMA. For accuracy, the best performance is obtained by our proposed forecasting system for the 30-min and 60-min intervals of wind speed with a MAPE of 5.36% and 6.64%, respectively. The highest value of RMSE is got by SVR for 60 min, and the highest value of other indicators is got by DES.

In addition, our proposed model outperforms all of the other models with regard to stability with a variance of error of 0.27 and 0.41, respectively. This is less than half those of the other models. This also shows that the DA obtained by our proposed model of above 0.75 is higher than that of other models, thus indicating that the future changes in wind speed can be better caught by our proposed system. In addition, very little difference exists between the three artificial neural networks, while the performance of DES is significantly poorer than ARIMA with regard to the statistical models.

4.2. Statistical hypothesis testing: Diebold-Mariano test

Hypothesis testing is a widely used method to infer a totality according to a sample in mathematical statistics based on certain assumptions [56].

In this paper, a hypothesis testing theory is introduced to verify the difference between the forecasting performances of the proposed model and competitive models. This theory is known as the Diebold-Mariano test [57].

Set a significant level α. The hypothesis test can be expressed as

$$H_0: E(d_i) = 0$$
$$H_1: E(d_i) \neq 0 \tag{15}$$

H_0 is the null hypothesis, indicating that there is no significant difference in the prediction performance between the proposed model and the competitive models. $d_m = L(e_i^{(1)}) - L(e_i^{(2)})$, where $L\ (x)$ is the arbitrary loss function of the forecasting error, which is calculated as $e_i^n = y_i - \hat{y}_i^{(n)},\ i = 1, 2...T, \quad n = 1, 2.$ $\{y_i,\ i = 1, 2, ..., T\}$ is the actual value of the time series, and $\{\hat{y}_i^{(n)},\ i = 1, 2, ..., T\}$ is the forecasting series for the same period of two different models.

Based on the definition of the above variance, the DM statistic can be defined as

$$DM = \frac{s^2 \sum_{i=1}^{T} (L(e_i^{(1)}) - L(e_i^{(2)}))/T}{\sqrt{s^2/T}} \tag{16}$$

where s^2 is the estimation of the variance of d_i. The DM test statistic can be regarded as standardized normal distribution N (0, 1). The null hypothesis will be rejected when $|DM| > Z_{\alpha/2}$, indicating that there is a difference between two models.

In this paper, a DM test is applied to test the difference between our proposed hybrid forecasting system and other models for three different sites and the time horizon wind speed. As it can be seen in Table 13, the minimum and maximum values of DM test are 2.69 and 14.27 respectively. According to the standard normal distribution table, $Z_{0.01/}$

Table 9
Comparison results of our proposed system with other competitive models.

Models		Proposed system	Artificial neural network			SVR	Statistical models		Persistence model
			BPNN	ELM	Elman		DES	ARIMA	
Site I	MAE	0.298760	0.496975	0.488415	0.708347	0.528708	0.751144	0.498261	0.528750
	RMSE	0.397983	0.677135	0.662338	0.947016	0.706443	1.045997	0.675638	0.723180
	MAPE (%)	3.839513	6.207713	6.155285	9.511818	6.683526	8.891636	6.212975	6.418183
	TIC	0.022445	0.038252	0.037410	0.054235	0.039909	0.058868	0.038130	0.040786
	DA	0.750853	0.550626	0.559727	0.497156	0.513083	0.395904	0.544937	0.000000
	VAR	0.158524	0.458959	0.439101	0.894897	0.499629	1.095355	0.456961	0.523532
Site II	MAE	0.305595	0.549370	0.541695	0.645208	0.624392	0.802402	0.526420	0.565682
	RMSE	0.400672	0.734510	0.720991	0.889162	0.889937	1.124607	0.692918	0.779525
	MAPE (%)	3.617997	6.318070	6.247136	7.237508	6.845307	8.947450	6.166419	6.420782
	U1	0.021281	0.039223	0.038455	0.048074	0.047818	0.059564	0.036820	0.041381
	DA	0.773606	0.544937	0.559727	0.506257	0.529010	0.385666	0.541524	0.000000
	VAR	0.160705	0.537661	0.518859	0.749929	0.771818	1.266178	0.480654	0.608301
Site III	MAE	0.304329	0.542251	0.538912	0.804627	0.599455	0.802390	0.529000	0.564886
	RMSE	0.404509	0.721916	0.717797	1.165756	0.818305	1.111845	0.703587	0.771208
	MAPE (%)	3.547821	6.122226	6.024588	9.186215	6.685766	8.688467	5.949024	6.176834
	U1	0.020822	0.037315	0.037075	0.061550	0.042424	0.057126	0.036258	0.039706
	DA	0.787258	0.563140	0.557452	0.500569	0.509670	0.392491	0.542662	0.000000
	VAR	0.163669	0.521270	0.515543	1.288847	0.664834	1.237605	0.495593	0.595383

Table 10
Comparison between single objective and multi-objectives.

Site I	MAE	RMSE	MAPE (%)	TIC	DA	VAR
EEMD-FTS-DE	0.304036	0.409553	3.874851	0.023091	0.750853	0.167802
EEMD-FTS-MODE	0.298760	0.397983	3.839513	0.022445	0.750853	0.158524
Site II	MAE	RMSE	MAPE (%)	TIC	DA	VAR
EEMD-FTS-DE	0.306735	0.402013	3.631538	0.021350	0.770193	0.161767
EEMD-FTS-MODE	0.305595	0.400672	3.617997	0.021281	0.773606	0.160705
Site III	MAE	RMSE	MAPE (%)	TIC	DA	VAR
EEMD-FTS-DE	0.306064	0.412478	3.543645	0.021234	0.782708	0.170247
EEMD-FTS-MODE	0.304329	0.404509	3.547821	0.020822	0.787258	0.163669

Table 11
Main wind speed forecasting horizons with their respective utilities for different sectors.

Wind speed forecasting horizons	Utilities in different sectors
Ultra-short term	Electricity market Real-time grid dispatch Regulation actions
Short term	Economic dispatch planning Make essential decisions Improve security in electricity market
Medium term	Decide unit commitment Determine reserve requirement Decide generator offline/online
Long term	Maintenance management Develop Operation plan Control operating cost Feasibility analysis for wind farm planning

$_2 = 2.58$, which is lower than the smallest value of |DM| in Table 13. From this, we conclude that the null hypothesis cannot be accepted at a 1% significance level. That is, our proposed hybrid forecasting system is significantly different from the other competitive models.

Considering the evaluation results in Section 3, the proposed hybrid system markedly improved the forecasting performance compared with other models for wind speed forecasting. Furthermore, it can be seen that the difference between the compared model and our proposed system decreases when the time interval increases, but a great difference still exists between the two models.

4.3. Forecasting effectiveness

In addition to some basic evaluation metrics such as MAE and MAPE, the forecasting effectiveness is introduced in this paper to evaluate the forecasting validity degree of models according to the sum of the squared errors and the forecasting accuracy's mean squared deviation. The expression form of the kth-order FE unit of the ith method is as follows:

$$m_i^k = \sum_{n=1}^{N} Q_n A_{in}^k$$

$$\sum_{n=1}^{N} Q_n = 1, \ Q_n > 0 \tag{17}$$

Q_n is the discrete probability distribution. Because prior information of the distribution cannot be known, Q_n is set as $1/N$. A_{in} is the forecasting accuracy of the ith method at time n, defined as

$$A_{in} = 1 - |\varepsilon_{in}| \tag{18}$$

$$\varepsilon_{in} = \begin{cases} -1, & (y_n - \hat{y}_{in})/y_n < -1 \\ (y_n - \hat{y}_{in})/y_n, & -1 \leqslant (y_n - \hat{y}_{in})/y_n < 1 \\ 1, & (y_n - \hat{y}_{in})/y_n > 1 \end{cases} \tag{19}$$

$H(m_i^1, m_i^2, \cdots, m_i^k)$ is defined as the k-order FE of the ith method. When $H(x) = x$ is a one-variable continuous function, $H(m^1) = m^1$ is the first-order FE that is the expected forecasting accuracy sequence. When $H(x, y) = x(1 - \sqrt{y - x^2})$ is a continuous function with two variables, the second-order FE that is the difference between the expectation and standard deviation can be expressed as

Table 12
Forecasting results of different methods for different wind speed intervals.

30 min	Fuzzy time series			SVR	Artificial neural network			Statistical model		Persistence model
	MODE	EW	EF		BPNN	ELM	Elman	DES	ARIMA	
MAE	0.388027	0.427459	0.459067	0.820103	0.672214	0.670214	0.705019	0.931453	0.665100	0.672500
RMSE	0.518051	0.553868	0.590006	1.168189	0.877737	0.872467	0.940989	1.212537	0.868658	0.882865
MAPE (%)	5.362977	6.065478	6.257845	10.699935	9.392999	9.245951	9.548770	12.313512	8.933546	9.185423
TIC	0.029159	0.031150	0.033106	0.066475	0.049473	0.049246	0.053274	0.067835	0.049095	0.049577
DA	0.796327	0.767947	0.732888	0.514190	0.542571	0.534224	0.542571	0.422371	0.522538	0.000000
VAR	0.268585	0.307282	0.348683	1.350865	0.771496	0.762051	0.885352	1.472700	0.752617	0.780747
60 min	Fuzzy time series			SVR	Artificial neural network			Statistical model		Persistence model
	MODE	EW	EF		BPNN	ELM	Elman	DES	ARIMA	
MAE	0.484242	0.536736	0.587426	1.156175	0.853316	0.855508	0.903452	1.170070	0.865180	0.866557
RMSE	0.641421	0.703568	0.754143	1.685688	1.097807	1.118190	1.204454	1.485795	1.117695	1.114215
MAPE (%)	6.639816	7.549227	7.881095	15.664036	12.269513	12.234222	12.782622	16.272534	11.723141	12.061317
TIC	0.036157	0.039676	0.042314	0.097146	0.062161	0.063392	0.068531	0.083090	0.062856	0.062680
DA	0.779605	0.766447	0.756579	0.492487	0.516447	0.549342	0.539474	0.434211	0.526316	0.000000
VAR	0.412612	0.496632	0.569016	2.796692	1.209143	1.254307	1.455274	2.214832	1.251772	1.245442

Table 13
DM test results between our proposed system and other models.

Datasets	Models	WFTS-EW	WFTS-EF	BPNN	ELM	Elman
Site I	Hybrid system	3.030741	6.370508	12.153724	11.898636	14.274400
Site II		3.384658	4.450159	12.885586	12.708539	12.435931
Site III		3.542094	5.604606	13.938883	13.582267	12.861968
30 min		3.540970	5.270023	11.225955	11.405091	10.365623
60 min		2.698111	4.27955	7.532328	7.532273	7.204769
Datasets	Models	SVR	DES	ARIMA	Persistence model	
Site I	Hybrid system	12.716411	13.544565	12.228671	12.787836	
Site II		10.337194	12.766318	13.007000	12.250042	
Site III		12.208821	13.590354	13.888870	13.071706	
30 min		8.195199	12.955963	11.154433	10.949072	
60 min		5.420146	8.965921	7.928481	7.955089	

$H(m^1, m^2) = m^1(1 - \sqrt{m^2 - (m^1)^2})$.

In this paper, FE is applied to compare the forecasting availability degrees of different methods. The model that possesses a greater FE has the better performance. The first-order FE is based on the forecasting accuracy sequence's expected value, and the second-order FE is based on the difference between its expected value and standard deviation. The values of the first- and second-order FEs are listed in Table 14.

We can see that the forecasting effectiveness will decrease when the time intervals increase. Thus, the best value is obtained by the 10-min wind speed time series. For the three sites with a 10-min time horizon, the best forecasting effectiveness is got at site II across all methods. Among these different models, the best forecasting effectiveness is obtained by our proposed hybrid forecasting system. For site I at a 10-min time interval, the first-order forecasting effectiveness of the proposed hybrid system, fuzzy time series with EW and EF, SVR, BPNN, ELM, Elman, DES, and ARIMA is 0.9616, 0.9558, 0.9523, 0.9332, 0.9379, 0.9384, 0.9049, 0.9111, and 0.9379, respectively, while the second-order forecasting effectiveness is 0.9293, 0.9212, 0.9137, 0.8800, 0.8872, 0.8879, 0.8131, 0.8430, and 0.8875, respectively.

4.4. Grey relational degree

The Grey relational degree is employed to measure the correlation level between the results of the different forecasting methods and actual time series [58].

Set $\{x_0(i)\}_{i=1}^{n}$ as the reference sequence, $\{x_j(i)\}_{i=1}^{n}$ as the comparative sequence, and $j = 1, 2, \ldots, m$. The relational coefficient of x_0 and x_j at point k is defined as

$$\xi_j(k) = \frac{\min_j \min_k |x_0(k) - x_j(k)| + \rho \max_j \max_k |x_0(k) - x_j(k)|}{|x_0(k) - x_j(k)| + \rho \max_j \max_k |x_0(k) + x_j(k)|} \tag{20}$$

ρ is the distinguishing coefficient, which is between 0 and 1, Here, ρ is set as 0.5. Then, the GRD is described as

$$r_i = \frac{1}{n} \sum_{k=1}^{n} \xi_{i(k)} \tag{21}$$

The GRD is used to measure the degree of correlation among different methods' forecasting results with actual wind speed time series [59]. The closer the forecasting value curves, the better the GRD value. From Table 15, it can be seen that our proposed hybrid forecasting system with its GRD at about 0.9 indicates that the forecasting value possesses the strongest correlation to the actual value. By contrast, the poorest GRD is obtained by DES of about 0.8 among these methods. For most models, the lowest values are obtained when the wind speed time series with 30-min intervals except for VAR.

4.5. The real application of our work

For practical application, accurate and stable forecasting of wind speed is a crucial theoretical and technical support for management and scheduling of power grid. In our study, a novel hybrid forecasting system is developed which can better balance the forecasting accuracy and stability to overcome wind-related uncertainty and guarantee the effective operation of smart grid [60]. Compare with the competitive models, improvement ratios of MAPE and VAR generated by our proposed system are above 50%. The more specific significance of a reliable and robust wind speed forecasting system is as follows:

(1) To rationally arrange maintenance plan and improve the effective use of time for wind power equipment. As far as we know, the wind turbines and other equipment in wind farm need to be regularly maintained and overhauled. According to the accurate wind speed forecast data, the maintenance and repair time of wind power

Table 14
Forecasting effectiveness of different models and intervals.

Models		Fuzzy time series			SVR	Artificial neural network			Statistical model		Persistence model
		MODE	EW	EF		BPNN	ELM	Elman	DES	ARIMA	
Site I	*First-Order*	0.961605	0.955798	0.952315	0.933165	0.937923	0.938447	0.904882	0.911084	0.937870	0.935993
	Second-Order	0.929264	0.921173	0.913661	0.880018	0.887188	0.887919	0.813145	0.843032	0.887492	0.885675
Site II	*First-Order*	0.963820	0.959643	0.959347	0.931547	0.936819	0.937529	0.927625	0.910525	0.938336	0.935924
	Second-Order	0.934910	0.928559	0.925035	0.878291	0.887837	0.888831	0.871095	0.840208	0.890652	0.884606
Site III	*First-Order*	0.964522	0.958977	0.957971	0.933142	0.938778	0.939754	0.908337	0.913115	0.940510	0.938123
	Second-Order	0.930483	0.925099	0.918106	0.876489	0.888834	0.891655	0.809735	0.845930	0.892835	0.888813
30 min	*First-Order*	0.946370	0.939345	0.937422	0.893018	0.906838	0.907540	0.905359	0.876865	0.908997	0.908323
	Second-Order	0.893371	0.880417	0.881626	0.799207	0.816420	0.820224	0.815291	0.780180	0.821676	0.824431
60 min	*First-Order*	0.933602	0.924508	0.921189	0.848734	0.881169	0.881150	0.876222	0.838336	0.880941	0.880282
	Second-Order	0.871700	0.850981	0.849549	0.726985	0.776509	0.775805	0.768008	0.715523	0.778060	0.777200

Table 15
Grey relational degree of different models and intervals.

Models	MODE	EW	EF	DES	ARIMA
Site I	**0.890288**	0.877870	0.876142	**0.786190**	0.835487
Site II	**0.903741**	0.894758	0.893889	**0.804749**	0.849925
Site III	**0.898128**	0.885651	0.881981	**0.792405**	0.840898
30 min	0.885038	0.874439	0.868444	0.780476	0.824039
60 min	0.897081	0.887991	0.881979	0.802236	0.835747
Models	SVR	BPNN	ELM	Elman	Persistence model
Site I	0.826811	0.835334	0.838413	0.816509	0.829350
Site II	0.830505	0.846636	0.846381	0.832643	0.844088
Site III	0.824929	0.839379	0.840188	0.788561	0.834802
30 min	0.791965	0.823512	0.821849	0.816037	0.822673
60 min	0.785911	0.836434	0.835156	0.832626	0.835843

equipment can be reasonably arranged. For example, the maintenance time of wind power equipment can be scheduled at low wind speed period which can effectively reduce the economic loss of power generation resulting from wind power equipment overhaul.

(2) To optimize power grid scheduling and reduce operation cost of power grid. Accurate forecasting of wind speed is the premise of wind power forecasting, which contributes to more accurately grasp the wind power output, and then provide the basis for the rational arrangement of power generation and scheduling plan for the power grid. Accurate wind speed prediction can improve the controllability of wind power, effectively reduce the reserve capacity of the power system, and foreseeingly arrange the start and stop of the wind turbine, so as to reduce the operation cost of the power system. For instance, the wind forecasting and its application in the scheduling of gas-fired generators was discussed by Xydas [61]. Ahmed indicated that long forecast horizons can be of significance for cost-effective energy management and dispatch strategies [57].

(3) To enhance power quality and strengthen wind power market competitiveness. Accurate forecasting of wind speed can improve the predictability of wind power and reduce the impact of wind power grid integration caused by the randomness and volatility of wind power. At the same time, when the forecast accuracy is used as an indicator for evaluating the power quality of wind farms by the power sector, the wind farm will pay more attention to the improvement of wind power quality to increase the competitiveness of wind power in the electricity market, and ultimately achieve a virtuous circle of wind power development and consumption.

5. Conclusion

Wind speed forecasting is a crucial contributor to the operational control of generator sets and improvements in the capacity of wind power integration. Accurate wind speed forecasting can alleviate the adverse effects of wind power on the power grid. However, wind speed in wind farms shows considerable randomness and non-stationarity, and the characteristics of wind speed vary greatly at different sites and under different time conditions. Thus, current wind speed forecasting is not very satisfactory but is essential nevertheless.

Using recent research and addressing current challenges, in this paper, a novel hybrid forecasting system was developed. This system performs excellent forecasting with wind speed time series. The “decomposition and ensemble” strategy in data preprocessing effectively reduces the noise pollution in the original data. The weight fuzzy time series, which takes advantage of fuzzy rules, is the main forecasting method in our system. Specifically, the multi-objective differential evolution algorithm referencing the multi-objective theory in a fitness function is applied to maintain the balance between conflicts of different evaluation metrics.

The proposed system is compared with some well-known traditional models and also the fuzzy time series method with different partition and optimization methods. The evaluation metrics indicated that future changes in wind speed can be well predicted by our proposed system which also shows great performance in forecasting accuracy and stability compared with other models. Moreover, statistical hypothesis testing, forecasting effectiveness, and grey relational degree analysis are carried out. These also proved the superiority of our proposed system. A comparison between different optimization algorithms found that multi-objective differential evolution algorithm outperforms the others in terms of evaluation metrics, statistical hypothesis testing, forecasting effectiveness, and grey relational degree.

An extension of our work includes conducting analyses during different time intervals of wind speed time series because of different demands from managers in different economic actives and sectors. The experimental results show that our proposed forecasting system significantly outperforms other methods during all time intervals. Furthermore, a wind speed time series with longer intervals obtained relatively poor performance, and the difference between different models thus decreased.

Conflict of interest

The authors declare that there is no conflict of interest regarding the publication of this paper.

Acknowledgements

This research was supported by the National Natural Science Foundation of China (Grant No. 71573034).

References

[1] Mathiesen BV, Lund H, Karlsson K. 100% Renewable energy systems, climate mitigation and economic growth. Appl Energy 2011;88:488–501.
[2] Fang G, Tian L, Fu M, Sun M, Du R, Lu L, et al. The effect of energy construction adjustment on the dynamical evolution of energy-saving and emission-reduction system in China ☆. Appl Energy 2017;196:180–9.
[3] Niu T, Wang J, Zhang K, Du P. Multi-step-ahead wind speed forecasting based on optimal feature selection and a modified bat algorithm with the cognition strategy. Renew Energy 2017.
[4] Dincer I, Acar C. Smart energy systems for a sustainable future. Appl Energy 2016;194.
[5] http://gwec.net/publications/global-wind-energy-outlook/global-wind-energy-outlook-2016/.
[6] http://gwec.net/global-figures/graphs/.
[7] http://www.indiaenvironmentportal.org.in/category/13410/publisher/global-wind-energy-council/.
[8] Ucar A, Balo F. Evaluation of wind energy potential and electricity generation at six locations in Turkey. Appl Energy 2009;86:1864–72.
[9] Monforti F, Gonzalez-Aparicio I. Comparing the impact of uncertainties on technical and meteorological parameters in wind power time series modelling in the European Union. Appl Energy 2017;206:439–50.
[10] Song J, Wang J, Lu H. A novel combined model based on advanced optimization algorithm for short-term wind speed forecasting. Appl Energy 2018;215:643–58. https://doi.org/10.1016/j.apenergy.2018.02.070.
[11] Jiang H, Wang J, Dong Y, Lu H. Comprehensive assessment of wind resources and the low-carbon economy: an empirical study in the Alxa and Xilin Gol Leagues of inner Mongolia, China. Renew Sustain Energy Rev 2015;50:1304–19.
[12] Allen DJ, Tomlin AS, Bale C, Skea A, Vosper S, Gallani ML, et al. A boundary layer scaling technique for estimating near-surface wind energy using numerical weather prediction and wind map data. Appl Energy 2017.
[13] Lei M, Luan S, Jiang C, Liu H, Yan Z. A review on the forecasting of wind speed and generated power. Renew Sustain Energy Rev 2009;13:915–20.
[14] Gao S, Dong L, Liao X, Gao YBT-CC. Very-short-term prediction of wind speed based on chaos phase space reconstruction and NWP 2013:8863–7.
[15] Tom H, Peter C. Correction and downscaling of NWP wind speed forecasts. Meteorol Appl 2010;14:105–16.
[16] Kavasseri RG, Seetharaman K. Day-ahead wind speed forecasting using f-ARIMA models. Renew Energy 2009;34:1388–93.
[17] Radziukynas V, Klementavicius ABT-ISC on P and EE of RTU. Short-term wind speed forecasting with ARIMA model 2014:145–9.
[18] Cadenas E, Rivera W. Wind speed forecasting in three different regions of Mexico, using a hybrid ARIMA-ANN model. Renew Energy 2010;35:2732–8. https://doi.org/10.1016/j.renene.2010.04.022.

[19] Yamaguchi A, Ishihara TBT-EA-PC on WE. Short term gust forecasting by using numerical weather prediction and multi timescale nonparametric regression model 2013:1083–6.
[20] Adamuthe AC, Gage RA, Thampi GTBT-IC on AC and CS. Forecasting cloud computing using double exponential smoothing methods; 2015.
[21] Chen L, Lai XBT-A-PP and EEC. Comparison between ARIMA and ANN models used in short-term wind speed forecasting 2011:1–4.
[22] Shukur OB, Lee MH. Daily wind speed forecasting through hybrid KF-ANN model based on ARIMA. Renew Energy 2015;76:637–47. https://doi.org/10.1016/j.renene.2014.11.084.
[23] Guo Z, Zhao W, Lu H, Wang J. Multi-step forecasting for wind speed using a modified EMD-based artificial neural network model. Renew Energy 2012;37:241–9. https://doi.org/10.1016/j.renene.2011.06.023.
[24] Zhang K, Qu Z, Wang J, Zhang W, Yang F. A novel hybrid approach based on cuckoo search optimization algorithm for short-term wind speed forecasting. Environ Prog Sustain Energy 2017;36.
[25] Liu H, Tian HQ, Liang XF, Li YF. Wind speed forecasting approach using secondary decomposition algorithm and Elman neural networks. Appl Energy 2015;157:183–94.
[26] Jiang P, Wang Y, Wang JZ. Short term wind speed forecasting by using a hybrid model. Energy 2017;119:561–77.
[27] Nieto PJG, García-Gonzalo E, Fernández JRA, Muñiz CD. Hybrid PSO–MARS–based model for forecasting a successful growth cycle of the Spirulina platensis from experimental data in open raceway ponds. Ecol Eng 2015;81:534–42.
[28] Liu H, Tian Hqi, Li Yfei. Comparison of two new ARIMA-ANN and ARIMA-Kalman hybrid methods for wind speed prediction. Appl Energy 2012;98:415–24. https://doi.org/10.1016/j.apenergy.2012.04.001.
[29] Okumus I, Dinler A. Current status of wind energy forecasting and a hybrid method for hourly predictions. Energy Convers Manag 2016;123:362–71. https://doi.org/10.1016/j.enconman.2016.06.053.
[30] Zhang W, Qu Z, Zhang K, Mao W, Ma Y, Fan X. A combined model based on CEEMDAN and modified flower pollination algorithm for wind speed forecasting. Energy Convers Manag 2017;136:439–51.
[31] Zhang M, Zhao S, Wang 2009. CEC '09. IEEE Congress on XBT-EC. Multi-objective evolutionary algorithm based on adaptive discrete differential evolution; 2009. p. 614–21.
[32] Deb K. Multi-objective genetic algorithms: problem difficulties and construction of test problems. Evol Comput 2014;7:205–30.
[33] Ameli A, Bahrami S, Khazaeli F, Haghifam MR. A multiobjective particle swarm optimization for sizing and placement of DGs from DG owner's and distribution company's viewpoints. IEEE Trans Power Deliv 2014;29:1831–40.
[34] Wang J, Heng J, Xiao L, Wang C. Research and application of a combined model based on multi-objective optimization for multi-step ahead wind speed forecasting. Energy 2017;125:591–613. https://doi.org/10.1016/j.energy.2017.02.150.
[35] Niazy RK, Beckmann CF, Brady JM, Smith SM. Performance evaluation of ensemble empirical mode decomposition. Adv Adapt Data Anal 2009. 01:0900010.
[36] Huang NE, Shen Z, Long SR, Wu MC, Shih HH, Zheng W, et al. The empirical mode decomposition method and the Hilbert spectrum for non-stationary time series analysis; 1998.
[37] Rilling G, Flandrin P, Goncalves P. On empirical mode decomposition and its algorithms. Proc IEEE-EURASIP work nonlinear signal image process NSIP-03, Grado (I 2003;3).
[38] Wu Z, Huang NE. Ensemble empirical mode decomposition: a noise-assisted data analysis method. Adv Adapt Data Anal 2005. 01:0900004.
[39] Yu L, Wang Z, Tang L. A decomposition – ensemble model with data-characteristic-driven reconstruction for crude oil price forecasting. Appl Energy 2015;156:251–67. https://doi.org/10.1016/j.apenergy.2015.07.025.
[40] Storn R, Price K. Differential evolution – a simple and efficient heuristic for global optimization over continuous spaces. J Glob Optim 1997;11:341–59. https://doi.org/10.1023/A:1008202821328.
[41] Price K, Storn RM, Lampinen JA, editors. Differential evolution: a practical approach to global optimization (Natural Computing Series). Springer-Verlag New York, Inc.; 2005.
[42] Islam S, Das S, Ghosh S. An adaptive differential evolution algorithm with novel mutation and crossover strategies for global numerical optimization. IEEE Trans Syst Man, Cybern Part B 2012;42:482–500. https://doi.org/10.1109/TSMCB.2011.2167966.
[43] Neri F, Tirronen VBT-EC. On memetic differential evolution frameworks: a study of advantages and limitations in hybridization; 2008. p. 2135–42.
[44] Mallipeddi R, Suganthan PN. Differential evolution algorithm with ensemble of 2010:71–8.
[45] Jehan MML. Differential evolution for multi-objective optimization 2003;031.
[46] Zadeh LA. The concept of a linguistic variable and its application to approximate reasoning – II. US: Springer; 1974.
[47] Song Q, Chissom BS. Fuzzy time series and its model. Fuzzy Sets Syst 1993;54:269–77.
[48] Song Q, Chissom BS. Forecasting enrollments with fuzzy time series — part II. Fuzzy Sets Syst 1994;62:1–8.
[49] Jiang P, Dong Q, Li P, Lian L. A novel high-order weighted fuzzy time series model and its application in nonlinear time series prediction. Appl Soft Comput J 2017;55:44–62. https://doi.org/10.1016/j.asoc.2017.01.043.
[50] Abdullah L, Taib I. High order fuzzy time series for exchange rates forecasting 2011:1–5.
[51] Wang J, Li H, Lu H. Application of a novel early warning system based on fuzzy time series in urban air quality forecasting in China. Appl Soft Comput 2018. https://doi.org/10.1016/j.asoc.2018.07.030.
[52] Chen S-M. Forecasting enrollments based on fuzzy time series. Fuzzy Sets Syst 1996;81:311–9. https://doi.org/10.1016/0165-0114(95)00220-0.
[53] Yang H, Jiang Z, Lu H. A hybrid wind speed forecasting system based on a "decomposition and ensemble" strategy and fuzzy time series. Energies 2017;10:1422. https://doi.org/10.3390/en10091422.
[54] Barbeito I, Zaragoza S, Tarrío-Saavedra J, Naya S. Assessing thermal comfort and energy efficiency in buildings by statistical quality control for autocorrelated data. Appl Energy 2017;190:1–17. https://doi.org/10.1016/j.apenergy.2016.12.100.
[55] Chang WY. A literature review of wind forecasting methods. J Power Energy Eng 2015;02:161–8.
[56] Du P, Wang J, Guo Z, Yang W. Research and application of a novel hybrid forecasting system based on multi-objective optimization for wind speed forecasting. Energy Convers Manag 2017;150:90–107. https://doi.org/10.1016/j.enconman.2017.07.065.
[57] Ahmed A, Khalid M. An intelligent framework for short-term multi-step wind speed forecasting based on Functional Networks. Appl Energy 2018;225:902–11. https://doi.org/10.1016/j.apenergy.2018.04.101.
[58] Sun S, Qiao H, Wei Y, Wang S. A new dynamic integrated approach for wind speed forecasting. Appl Energy 2017;197:151–62. https://doi.org/10.1016/j.apenergy.2017.04.008.
[59] Zheng G, Jing Y, Huang H, Gao Y. Application of improved grey relational projection method to evaluate sustainable building envelope performance. Appl Energy 2010;87:710–20.
[60] Watson SJ, Landberg L, Halliday JA. Application of wind speed forecasting to the integration of wind energy into a large scale power system. IEE Proc – Gener Transm Distrib 1994;141:357–62.
[61] Xydas E, Qadrdan M, Marmaras C, Cipcigan L, Jenkins N, Ameli H. Probabilistic wind power forecasting and its application in the scheduling of gas-fired generators. Appl Energy 2017;192:382–94. https://doi.org/10.1016/j.apenergy.2016.10.019.